

# The use and calibration of read-out streaks to increase the dynamic range of the *Swift* Ultraviolet/Optical Telescope

M. J. Page,<sup>1\*</sup> N. P. M. Kuin,<sup>1</sup> A. A. Breeveld,<sup>1</sup> B. Hancock,<sup>1</sup> S. T. Holland,<sup>2</sup>  
F. E. Marshall,<sup>3</sup> S. Oates,<sup>1</sup> P. W. A. Roming,<sup>4,5</sup> M. H. Siegel,<sup>5</sup> P. J. Smith,<sup>1</sup>  
M. Carter,<sup>1</sup> M. De Pasquale,<sup>1</sup> M. Symeonidis,<sup>1</sup> V. Yershov<sup>1</sup> and A. P. Beardmore<sup>6</sup>

<sup>1</sup>Mullard Space Science Laboratory, University College London, Holmbury St Mary, Dorking, Surrey RH5 6NT, UK

<sup>2</sup>Space Telescope Science Centre, 3700 San Martin Drive, Baltimore, MD 21218, USA

<sup>3</sup>Astrophysics Science Division, Code 660.1, Goddard Space Flight Center, 8800 Greenbelt Road, Greenbelt, MA 20771, USA

<sup>4</sup>Space Science & Engineering Division, Southwest Research Institute, PO Drawer 28510, San Antonio, TX 78228-0510, USA

<sup>5</sup>Department of Astronomy & Astrophysics, Penn State University, 525 Davey Laboratory, University Park, PA 16802, USA

<sup>6</sup>Department of Physics and Astronomy, University of Leicester, Leicester LE1 7RH, UK

Accepted 2013 September 4. Received 2013 August 31; in original form 2013 May 14

## ABSTRACT

The dynamic range of photon counting micro-channel-plate (MCP) intensified charged-coupled device (CCD) instruments such as the *Swift* Ultraviolet/Optical Telescope (UVOT) and the *XMM–Newton* Optical Monitor (XMM-OM) is limited at the bright end by coincidence loss, the superposition of multiple photons in the individual frames recorded by the CCD. Photons which arrive during the brief period in which the image frame is transferred for read out of the CCD are displaced in the transfer direction in the recorded images. For sufficiently bright sources, these displaced counts form read-out streaks. Using UVOT observations of Tycho-2 stars, we investigate the use of these read-out streaks to obtain photometry for sources which are too bright (and hence have too much coincidence loss) for normal aperture photometry to be reliable. For read-out-streak photometry, the bright-source limiting factor is coincidence loss within the MCPs rather than the CCD. We find that photometric measurements can be obtained for stars up to 2.4 mag brighter than the usual full-frame coincidence-loss limit by using the read-out streaks. The resulting bright-limit Vega magnitudes in the UVOT passbands are UVW2 = 8.80, UVM2 = 8.27, UVW1 = 8.86,  $u$  = 9.76,  $b$  = 10.53,  $v$  = 9.31 and White = 11.71; these limits are independent of the windowing mode of the camera. We find that a photometric precision of 0.1 mag can be achieved through read-out streak measurements. A suitable method for the measurement of read-out streaks is described and all necessary calibration factors are given.

**Key words:** space vehicles: instruments – techniques: photometric – ultraviolet: general.

## 1 INTRODUCTION

The Ultraviolet/Optical Telescope (UVOT; Roming et al. 2005) is a 30 cm optical/UV telescope mounted on the NASA *Swift* observatory (Gehrels et al. 2004). The UVOT is coaligned with the X-ray Telescope (XRT; Burrows et al. 2005) on a rapidly repointing satellite bus so that the two instruments can observe the afterglows of gamma-ray bursts within two minutes of a gamma-ray burst being detected by the wide-field Burst Alert Telescope (BAT; Barthelmy et al. 2005).

The UVOT is of a modified Ritchey Chrétien design. After reflections on the primary and secondary mirrors, the incoming light passes through a hole in the primary to a flat tertiary mirror which directs the light to one of two identical filter wheel and detector chains. There are seven imaging filters mounted in the UVOT filter wheel together with two grisms for low-dispersion spectroscopy. Three optical filters,  $u$ ,  $b$  and  $v$ , cover similar wavelength ranges to the Johnson UB $V$  set (Johnson & Morgan 1951), and three UV filters, UVW2, UVM2 and UVW1, have central wavelengths of 1928 Å, 2246 Å and 2600 Å, respectively. The remaining filter, White, transmits over the full UVOT bandpass (1600–8000 Å) to maximize throughput.

The UVOT detector is a micro-channel plate (MCP) intensified charge coupled device (CCD) (MIC; Fordham et al. 1989).

\* E-mail: mjp@mssl.ucl.ac.uk

Individual incident photons liberate electrons in a multi-alkali (S20) photo-cathode, which are multiplied a million-fold using MCPs in series. These electrons strike a phosphor screen, producing photons which are fed to the CCD via a fibre-optic taper. The resulting cascade of photons arriving on the CCD is centroided on-board to a precision of one eighth of a CCD pixel. The  $256 \times 256$ -pixel science area of the CCD thus localizes individual incoming photons on a grid of  $2048 \times 2048$  pixels of size  $0.5 \text{ arcsec} \times 0.5 \text{ arcsec}$  with a time resolution equal to the frame time of the CCD (usually  $11.0329 \text{ ms}$ ). The onboard centroiding produces a low-level modulo-8 fixed-pattern distortion (Kawakami et al. 1994) which is routinely corrected in the ground processing. Data are recorded and transmitted to the ground as an event list, in which the arrival times and positions of individual photons are recorded, or as an image accumulated over a timed exposure. To reduce data volume, images are often binned by a factor of 2 in  $x$  and  $y$  before transmission to the ground.

The *Swift* UVOT has an almost identical optical design and a similar detector system to the *XMM-Newton* Optical Monitor (XMM-OM; Mason et al. 2001). The XMM-OM differs from the UVOT mainly in its UV throughput (which is lower in XMM-OM), its control and data processing computers (which are of an earlier vintage in XMM-OM) and in its operating modes.

The detector response is asymptotically linear when the arrival rate of photons is small compared to the CCD readout frame rate. In normal operation the UVOT has a frame rate of  $90.6 \text{ s}^{-1}$  although modes with higher frame rates which read out only a subset of the detector are available. For sources with count rates that are an appreciable fraction of the frame rate, two or more photons may arrive at a similar location on the detector within the same CCD frame, and are counted as a single photon. This phenomenon is known as coincidence loss (Fordham, Moorhead & Galbraith 2000b) and is analogous to pile-up in X-ray CCD detectors. Source count rates are routinely corrected for coincidence loss in the UVOT tasks in the *HEASOFT* *Swift* *FTOOLS* software package,<sup>1</sup> and details of the corrections are described in Poole et al. (2008) and Breeveld et al. (2010). The finite number of frames in an exposure implies that the measured count rate follows a binomial (rather than Poisson) distribution, and as the source count rate approaches the frame rate of the CCD the photometric measurement errors become larger rather than smaller (Kuin & Rosen 2008). The coincidence-loss correction has been calibrated up to 0.96 detected counts per frame (before correction for coincidence loss) in a 5 arcsec radius circular aperture (Poole et al. 2008), corresponding to a corrected count rate of  $300 \text{ s}^{-1}$  in full-frame mode, beyond which coincidence loss can no longer be accurately corrected, and this can be taken to define the upper limit to the dynamic range of UVOT.

Once per CCD frame the charge is transferred vertically to the read-out section. Sources add counts to parts of the image that pass below them on the detector while the charge is being transferred, so that bright sources give rise to vertical lines of enhanced brightness on the image, aligned with the bright sources. These lines are commonly known as read-out streaks<sup>2</sup> (see Fig. 1).

In this paper we describe how the read-out streaks can be used to make photometric measurements with UVOT of stars which are too

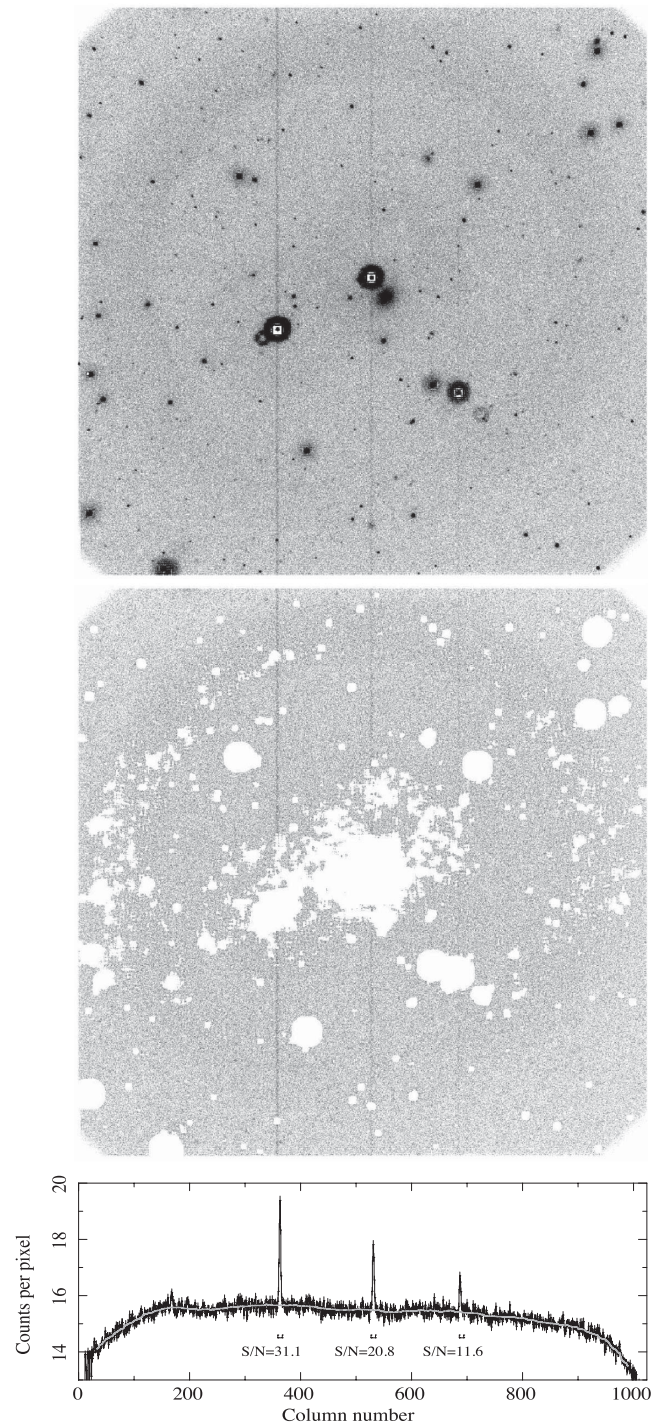


**Figure 1.** Illustration of the measurement process for read-out streaks. Top panel: raw  $v$ -band image from observation number 00030875001. The image was binned onboard the spacecraft by a factor of 2 in  $x$  and  $y$ , as is common for UVOT images. A logarithmic colour table has been employed to emphasize faint features including the read-out streaks. Middle panel: the same image after bright stars and features have been masked, as described in Section 3.2. Bottom panel: the mean pixel brightness in each column of the masked image. The grey line shows the 128-column median which is used for background estimation. The read-out streaks from the three brightest stars are significantly detected. The apertures used to measure the brightness of the streaks are shown below them, and labelled with the signal-to-noise ratios.

<sup>1</sup> *HEASOFT* software can be found at: <http://heasarc.gsfc.nasa.gov/docs/software/lheasoft/>

<sup>2</sup> X-ray astronomers will note that the streaks of out-of-time events seen in X-ray CCD cameras are formed in an analogous process to the read-out streaks in UVOT.

bright to be measured through aperture photometry at the position of the star on the image. While the calibration obtained and verified in this paper is specific to the UVOT, the principles apply equally to the XMM-OM.

The paper is laid out as follows. Section 2 outlines the basic principles behind photometry using read-out streaks. The catalogue of objects of known magnitudes which are used to investigate photometry using read-out streaks and the method we adopt to measure them are described in Section 3. The results of our investigation are presented in Section 4. We discuss these results and develop a method to measure photometry using read-out streaks in any UVOT passband and window mode in Section 5. A demonstration of the method is provided in the form of early-time photometry of the exceptionally bright gamma-ray burst GRB 080319B. Our conclusions are presented in Section 6. A step-by-step description of our recommended procedure to derive photometry from read-out streaks is given in Appendix A.

## 2 PRINCIPLES OF PHOTOMETRY USING READ-OUT STREAKS IN THE UVOT

The UVOT detector employs an EEV CCD-02-06 frame-transfer CCD. At the end of the integration period of each CCD frame, charge is transferred from the imaging area to the frame-store in 290 steps, each taking 600 ns. The read-out streaks are formed during this 174  $\mu$ s interval; as only 256 of the 290 rows correspond to the science imaging area, the effective exposure time of a complete 256-row read-out streak is 153.6  $\mu$ s per frame. For comparison, in full-frame operation, the live exposure time (i.e. excluding the frame-transfer time) per 11.0329 ms frame is 10.8589 ms, so that the complete 256-row read-out streak would be expected to contain 0.01415 times as many counts as the corresponding object in the direct image. As the exposure is uniform at all points along the read-out streak the streak will have uniform brightness in the vertical direction. The speed at which the image is transferred through the CCD is sufficiently large that coincidence loss should be much less of a problem than in the direct image: the effective count rate for coincidence loss is reduced by the ratio of counts in the streak to the direct image divided by the extent of the streak in CCD rows relative to the size of a photon splash. Thus if a photon splash is considered to cover 3 pixels, this means that the effective count rate for coincidence loss will be  $0.01415 \times 3/256 = 1.7 \times 10^{-4}$  the count rate of the source in the direct image, implying a  $>9$  mag advantage in the bright limit for photometric measurement with respect to the direct image. However, coincidence loss arising in a different part of the detector is expected to intervene well before such a large dynamic range is achieved. Charge is stripped from pores of the MCPs during the electron amplification, and the time-scale for the pores of the MCPs in the intensifier to recharge after ejecting electrons is of the order of 0.3 ms. This dead-time in the MCP pores following an event may become the limiting factor by giving rise to a second level of coincidence loss, which is independent of the CCD (Fordham et al. 2000a).

## 3 METHOD

### 3.1 Input catalogue

Investigation of the read-out streaks for photometry requires the measurement of the read-out streaks of a sufficient sample of stars, covering an appropriate magnitude range, with known magnitudes in a photometric system which can be related systematically to that

of the UVOT. We decided to use stars from the Tycho-2 catalogue which fall serendipitously within the fields of view of archival full-frame  $v$ -band UVOT observations. To avoid issues related to image crowding, we selected observations at Galactic latitudes of  $b > 20^\circ$  so as to exclude the Galactic Plane and Magellanic Clouds. The Tycho-2 catalogue (ESA 1997) contains 2.5 million stars with photometry in two bands from the sky mapper of the ESA *Hipparcos* satellite. The Tycho-2  $V_T$  passband covers a similar wavelength range to the UVOT  $v$  band, and in combination with the Tycho-2  $B_T$  magnitudes a suitable transformation to UVOT  $v$ -band photometry can be made (see Section 3.3). The Tycho-2 catalogue contains stars with a wide range of magnitudes with reliable photometry down to  $V_T = 12$  mag (Høg et al. 2000), which is approximately the limit to which read-out streaks can be easily measured in UVOT images.

To avoid problems with the transformation between Tycho-2 photometry and UVOT  $v$  (see Section 3.3), we excluded stars of spectral type M from our analysis. Discrimination of M stars from stars of earlier spectral type is poor using Tycho-2  $B_T - V_T$  colour, so we cross-correlated our sample of Tycho-2 stars with the Two Micron All Sky Survey (2MASS; Skrutskie et al. 2006). Stars with  $V_T - J > 3.0$  are likely to be M stars and were excluded from our sample. After these stars were excluded, we measured the read-out streaks for a total of 160 stars.

### 3.2 Measurement of read-out streaks

Read-out streaks are precisely vertical in raw UVOT images, but this is not the case after images have been corrected for distortion (primarily from the fibre taper connecting the phosphor screen to the CCD) and rotated so that  $x$  and  $y$  coordinates correspond to equatorial coordinate axes. Therefore read-out streaks are best measured from the raw UVOT images, after correction for modulo-8 noise, but before the distortion corrections. In practice the read-out streak can never be measured over the full vertical extent of the image because the direct image of the star responsible for the read-out streak, and any other stars which are located in the same column, will be superimposed on it. Therefore the brightness of the streak must be measured from parts of the streak which are not contaminated by objects in the image.

The brightness of the read-out streaks was measured according to the following procedure. Note that in the description that follows, the terms pixel, row and column refer to unbinned UVOT image pixels, rows and columns of image pixels, respectively. First, bright sources with count rates exceeding 40 count  $s^{-1}$  were identified in the image and masked with circular regions of radius 24 arcsec. This separate step is needed for bright stars because they are surrounded by dark regions which result from coincidence loss, which would not be identified in a regular source searching process. Next, each column of the image was searched for enhanced-brightness pixels corresponding to sources in two steps. First, individual pixels exceeding the median pixel value of the column by more than  $3\sigma$ , or by more than three counts if the median of the column is  $\leq 1$ , are flagged. In the second step, the column is smoothed with a 10-pixel boxcar filter to improve sensitivity to faint sources before again flagging pixels which exceed the median of the column by more than  $3\sigma$ , or by more than three counts if the median of the column is  $\leq 1$ . Pixels flagged in either step are then masked from the column. The rationale for performing this operation column by column rather than simply source-searching the image is that it prevents the read-out streaks themselves from being erroneously identified as sources. Next, the columns are collapsed to a single row containing, for each column, the mean value of all non-masked pixels in

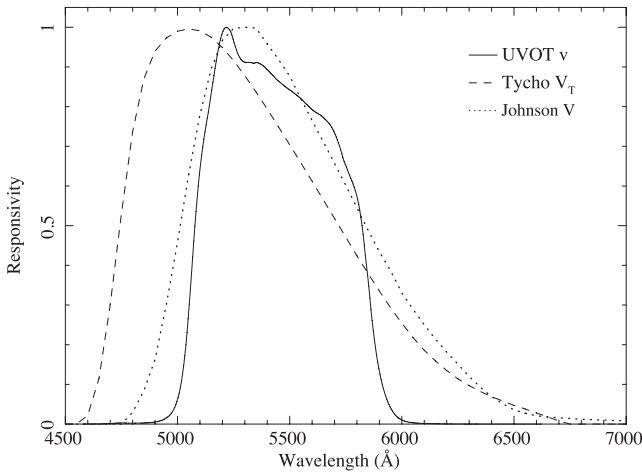


**Figure 2.** Responsivity curves for the UVOT  $v$  (solid line), Tycho-2  $V_T$  (dashed line) and Johnson  $V$  (dotted line) passbands.

the column. Read-out streaks are then identified using a 16-column sliding box along the row, at a 6-sigma threshold with respect to the median counts measured in a 128-column sliding box. The count rate in the 16-pixel aperture is then background-subtracted using the 128-column median, and scaled to a 16-row section of the image (i.e. multiplied by a factor of 16 assuming an unbinned image). The scaling in this stage is arbitrary, but 16 pixels  $\times$  16 pixels is a convenient equivalent aperture in which to measure the count rate of the read-out streak because it has a similar sky area to the 5 arcsec radius circular aperture normally used for photometry of point sources in UVOT images,<sup>3</sup> as well as corresponding to precisely  $2 \times 2$  CCD pixels (which are subsampled by a factor of 8 in the event centroiding process, as described in Section 1). The size of the 128-pixel sliding box used for background is chosen as a compromise between tracing the variation in background over the image (see Fig. 1) and minimizing the contribution of the background estimation to the statistical uncertainty of the read-out streak measurement. Finally, the count rate of the read-out streak is corrected for the large-scale sensitivity variations (evaluated at the position of the star in the image) and time-dependent sensitivity degradation of the UVOT (Breeveld et al. 2010).

### 3.3 Transformation from the Tycho-2 to UVOT photometric system

Responsivity curves for the UVOT  $v$  band, Johnson  $V$  band and Tycho-2  $V_T$  band are shown in Fig. 2. While all three cover approximately the same wavelength range, there are significant differences in the shapes of the curves, so that translation between the different photometric systems is colour-dependent. To derive a transformation between Tycho-2  $V_T$  and UVOT  $v$  magnitudes, we generated synthetic  $B_T - V_T$  and  $v - V_T$  colours for the stars of the Pickles (1998) spectral library. Fig. 3 shows the resulting colour-colour distribution for spectral types K and earlier. For stars with  $B_T - V_T > 0$

<sup>3</sup> The sky area of the aperture used for measuring the read-out streaks is slightly smaller than that used for aperture photometry of point sources in the image, but this difference is offset by the lossless redistribution of photons in the vertical direction in the read-out streak: photons in the wings of the point-spread function are not lost from the read-out streak when they are displaced in the vertical direction.

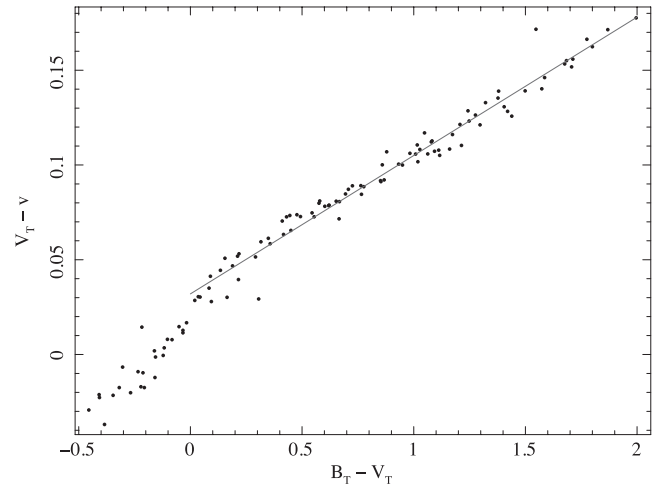


**Figure 3.** Difference between UVOT  $v$  and Tycho-2  $V_T$  magnitudes as a function of Tycho-2  $B_T - V_T$  colour. The points correspond to synthetic photometry of stars from the (Pickles 1998) spectral atlas. Stars of spectral type M are not shown. The grey line shows the fit to the data from which the colour transformation given in Section 3.3 is derived.

there is a tight linear relation between  $B_T - V_T$  and  $v - V_T$ . From a least-squares fit to the data points with  $B_T - V_T > 0$  (shown as a grey line in Fig. 3) we obtain the following transformation:

$$v = V_T - 0.032 - 0.073(B_T - V_T). \quad (1)$$

The rms scatter of the data points about this relation is 0.006 mag for  $B_T - V_T > 0$ . Stars with  $B_T - V_T < 0$  deviate from this linear relation, but this is not of concern because all of the Tycho-2 stars used in our read-out streak analysis have  $B_T - V_T > 0$ .

Stars of spectral type M were not used to derive the colour transformation because they show a much larger scatter in the  $B_T - V_T$  and  $v - V_T$  relation than stars of earlier spectral type; a similar problem besets the transformation of Tycho-2 magnitudes to Johnson  $V$  (ESA 1997).

## 4 RESULTS

Fig. 4 shows the relation between  $v$  magnitude derived from Tycho-2 and the count rate of the read-out streak in a 16 pixel  $\times$  16 pixel aperture for the sample of Tycho-2 stars observed in full-frame UVOT  $v$ -band images. As described in Section 2, the fixed ratio of exposure time in the read-out streak and the static image implies that the read-out streak will receive 0.01415 times as many counts as the direct image. This ratio must be divided by a factor of 128 to scale to a 16 pixel section of the read-out streak (corresponding to our 16 pixel  $\times$  16 pixel aperture), so that the zero-point appropriate to convert read-out-streak count rate to magnitude in such an aperture will be 9.89 mag brighter than the corresponding zero-point used for aperture photometry of the static image; for the  $v$  band of UVOT this implies a zero-point of 8.00 for photometry using the read-out streak. The dashed line in Fig. 4 shows the count rate to magnitude relation predicted from this zero-point. While the measured count rates are clustered around the predicted relation at the faintest magnitudes ( $v > 11$ ), they are systematically below it at brighter magnitudes. For  $v < 8$  the count rates show a large scatter and show little correlation with the magnitude of the source. As described in Section 2, these magnitudes are not bright enough for the diminished count rates to be due to coincidence loss on the

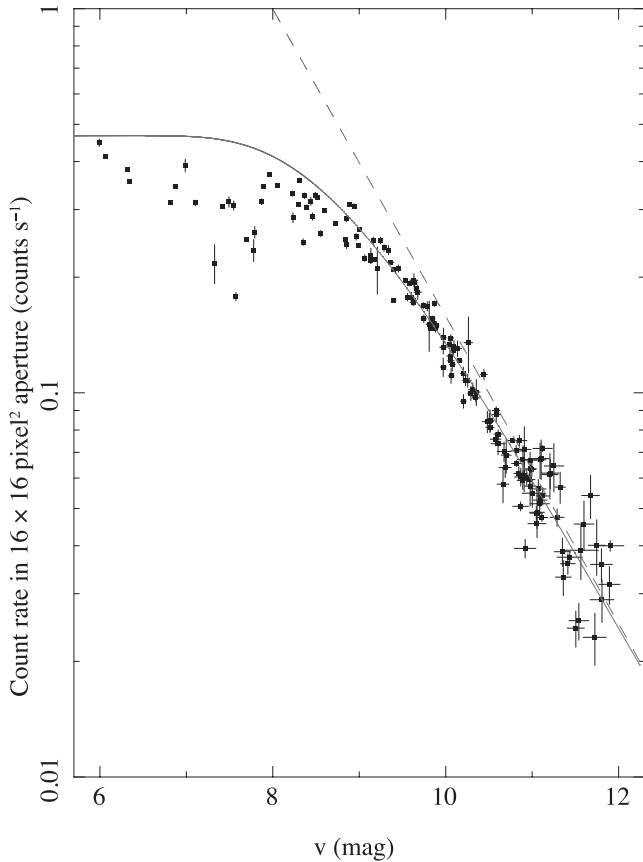


**Figure 4.** Count rates of the read-out streaks originating from Tycho-2 stars measured in a  $16 \times 16$  pixel aperture. The grey dashed line corresponds to the predicted relation given in Section 2 based on the relative exposure times of the read-out streak and the static image; it is not a fit to the data. The grey solid line shows the expected relation in the presence of coincidence loss as described by equation (3) with  $t_{\text{MCP}} = 2.36 \times 10^{-4}$  s.

CCD during frame transfer. A more likely culprit is the coincidence loss of photons which arrive while the MCP pores are recharging, predicted by Fordham et al. (2000b). As this coincidence loss arises in the MCPs rather than the CCD, it is independent of the CCD frame time. We can assume that by the third in-series MCP in the intensifier, the area of the MCP which is utilized in the detection of incoming photons from a point source is large enough that the process can be treated as coincidence loss in a single-pixel detector. Starting from equation (4) of Fordham et al. (2000b)

$$C_o = 1 - e^{-C_i} \quad (2)$$

where  $C_o$  is the mean number of counts observed per frame (i.e. after coincidence loss) and  $C_i$  is the mean number of incoming counts per frame (i.e. before coincidence loss). In this case a frame is the time-scale required for the MCP to recharge, which we will call  $t_{\text{MCP}}$ , and all counts from the source contribute to coincidence loss, not just those which arrive during the formation of the read-out streak. If the ratio of the integration time of the static image to the frame-transfer time is  $S$ , the count rate of a source in the static image will be  $S$  times the count rate that will be measured in a  $16 \times 16$  pixel section of the read-out streak. Hence the numbers of counts per frame are related to the count rates before and after correction for coincidence loss as

$$C_i = SR_i t_{\text{MCP}}$$

**Table 1.** Characteristics of the full-frame and windowed operating modes of UVOT that are important for read-out streak photometry.  $S$  is the ratio of the static image exposure time to the frame-transfer exposure time (see Section 4). Max count rate refers to the maximum coincidence-loss-corrected count rate of a read-out streak in a  $16 \times 16$  pixel aperture for which we recommend using read-out streak photometry.

Window mode	CCD frame time (ms)	$S$	Max count rate ( $\text{s}^{-1}$ )
Full frame	11.0329	9049	0.30
Large window	5.417	4369	0.62
Small window	3.600	2855	0.95

and

$$C_o = SR_o t_{\text{MCP}},$$

respectively, where  $R_i$  is the incoming count rate in a  $16 \times 16$  pixel section of the read-out streak before coincidence loss and  $R_o$  is the observed count rate with coincidence loss. Substituting and rearranging, we obtain

$$R_o = \frac{1 - e^{-(SR_i t_{\text{MCP}})}}{S t_{\text{MCP}}}. \quad (3)$$

The values of  $S$  corresponding to the full-frame and windowed operating modes of UVOT are given in Table 1.

As the time-scale for MCP recharge  $t_{\text{MCP}}$  is not known a priori, we performed a  $\chi^2$  fit to the data in Fig. 4. In the fitting, magnitude uncertainties on the Tycho-2 stars were translated into count rate uncertainties and added in quadrature to the measurement errors on the count rates. Stars brighter than  $v = 9$ , for which the read-out streaks exhibit an increasing degree of scatter with brightness, were excluded from the fit. The fitting yields a best-fitting  $t_{\text{MCP}} = 2.36 \pm 0.03 \times 10^{-4}$  s. The relation for count rate against magnitude corresponding to  $t_{\text{MCP}} = 2.36 \times 10^{-4}$  s is shown as the solid curve in Fig. 4. It reproduces the overall trend of the data well for sources fainter than 9th magnitude and the apparent count rate ceiling at  $\sim 0.45 \text{ s}^{-1}$ . However, coincidence loss does not explain the large scatter in count rates seen for sources with  $v < 8$ . There are (at least) two possible causes for this large scatter at bright magnitudes. It might be due to the electron wells of the CCD becoming over-full, leading to charge bleeding into the relevant CCD column so that individual photon splash events can no longer be identified as the frames are read out; the degree to which counts are lost might depend on the positioning of the source in the field of view, and/or with respect to the boundaries of the CCD columns. Alternatively, it could be due to variations of the electron mobility with position on the MCPs, perhaps as a result of local ageing of the MCPs (which would imply a dependence on time as well as position). Whatever the cause, no useful information on source brightness can be gleaned from the read-out streaks for sources brighter than magnitude 8 in  $v$ .

Rearranging equation (3) we obtain:

$$R_i = -\frac{\log_e(1.0 - (SR_o t_{\text{MCP}}))}{S t_{\text{MCP}}} \quad (4)$$

which can be used together with our best-fitting  $t_{\text{MCP}} = 2.36 \times 10^{-4}$  s to correct the measured count rate in the read-out streak for coincidence loss. Fig. 5 shows the corrected count rates for the Tycho-2 stars against their  $v$  magnitudes. As in Fig. 4, the dashed line gives the expected relation between

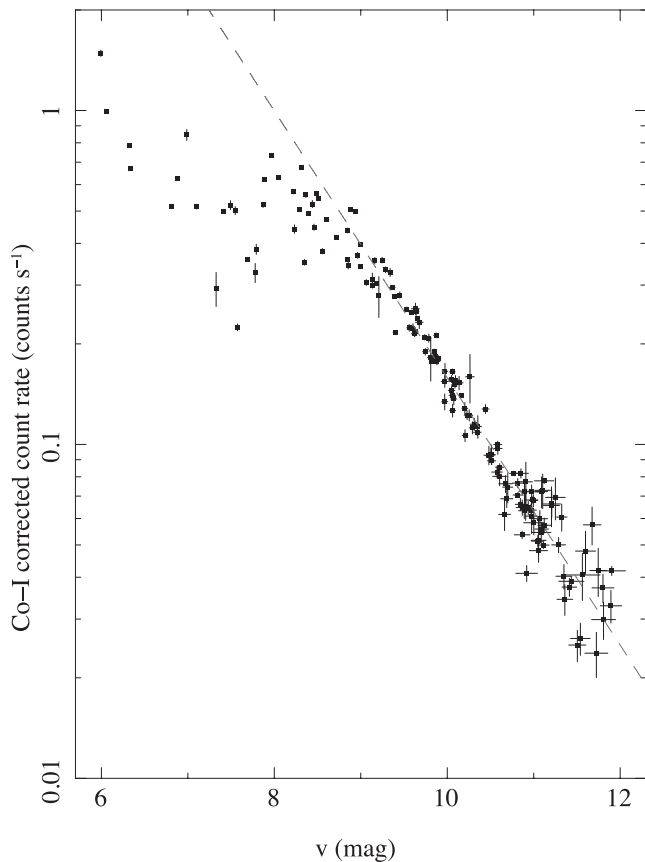


**Figure 5.** Count rates of the read-out streaks originating from Tycho-2 stars measured in a  $16 \text{ pixel} \times 16 \text{ pixel}$  aperture after correction for coincidence loss via equation (4) and  $t_{\text{MCP}} = 0.236 \text{ ms}$ . As in Fig. 4, the dashed line corresponds to the predicted relation given in Section 2 based on the relative exposure times of the read-out streak and the static image.

magnitude and count rate. The coincidence-loss-corrected count rates trace the dashed line well for  $v > 9 \text{ mag}$ . We now look in more detail at the photometric precision which might be achieved using read-out streak measurements. The top panel of Fig. 6 shows the differences  $\Delta m$  between the  $v$  magnitudes derived from the Tycho-2 magnitudes and the  $v$  magnitudes obtained from the coincidence-loss-corrected read-out streak measurements as a function of  $v$  magnitude (from Tycho-2) of the individual stars. The uncertainties on  $\Delta m$  are the sums in quadrature of the Tycho-2 and UVOT uncertainties.

To look for any systematic trends of photometry with magnitude and to estimate the level of photometric precision that can be achieved through measurements of the read-out streaks, we have used the maximum-likelihood approach outlined by Maccararo et al. (1988) to measure the mean and intrinsic standard deviation of the  $\Delta m$  distribution (which we assume to be Gaussian), taking into account the measurement errors, in half-magnitude bins. The means are shown in the middle panel of Fig. 6 and do not show any systematic trend with magnitude. Except for the faintest magnitude bin, where the error is larger, the mean values of  $\Delta m$  ( $\langle \Delta m \rangle$ ) are within  $\pm 0.05 \text{ mag}$  of  $\langle \Delta m \rangle = 0$ ; the faintest magnitude bin is consistent with  $\langle \Delta m \rangle = 0$  within its uncertainty. Over the full  $9 < v < 12 \text{ mag}$  range  $\langle \Delta m \rangle = -0.005 \pm 0.005$ . The standard deviations  $\sigma_{\Delta m}$  are shown in the bottom panel. Apart from the faintest magnitude bin (which again has a larger uncertainty than the others) the best-fitting

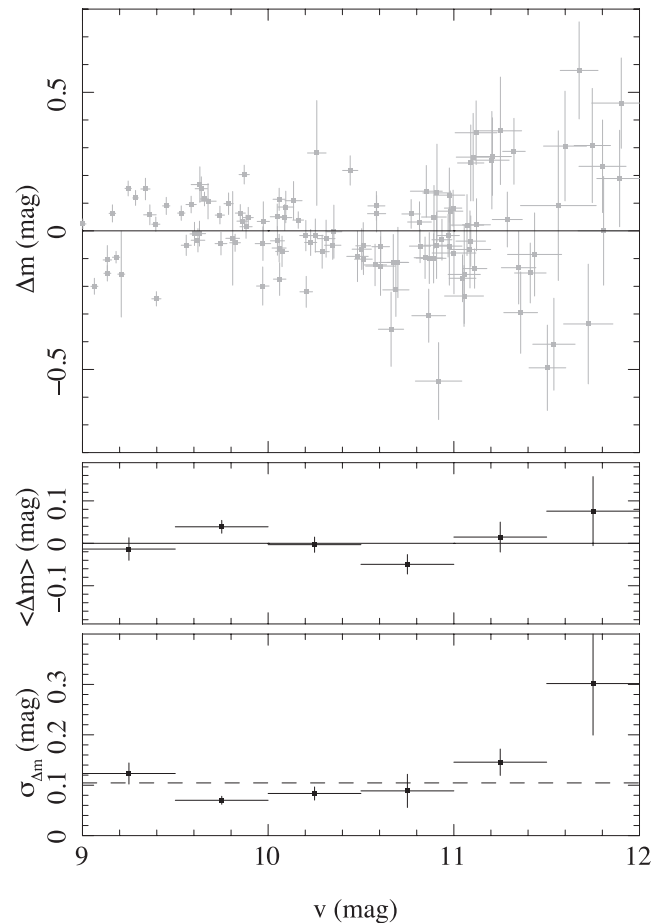


**Figure 6.** Top panel: differences  $\Delta m$  between the  $v$  magnitudes obtained from Tycho-2 and the  $v$  magnitudes obtained from the coincidence-loss corrected count rates of the UVOT read-out streaks. Uncertainties are the quadrature sums of the errors on the count rates and the Tycho-2 magnitudes. Middle and bottom panels: mean and dispersion of  $\Delta m$ , respectively, in  $0.5 \text{ mag}$  bins. The dashed line in the bottom panel shows the best-fitting dispersion over the full  $9 < v < 12 \text{ mag}$  interval shown.

values of  $\sigma_{\Delta m}$  are between  $0.07$  and  $0.13 \text{ mag}$ . Over the full magnitude range, the best-fitting  $\sigma_{\Delta m} = 0.104 \pm 0.004 \text{ mag}$ , and this is shown in the bottom panel of Fig. 6 as a dashed line. This  $\sigma_{\Delta m}$  represents the systematic error on the read-out streak photometry which remains after the statistical uncertainty is accounted for.

## 5 DISCUSSION

### 5.1 Using read-out streaks for photometry

The use of UVOT read-out streaks for photometry relies on the calibration or knowledge of four instrumental properties: the effective area as a function of wavelength, the zero-point for direct imaging, the ratio of exposure times between the read-out streak and the static image in the CCD, and the effective recharge time-scale for the MCP intensifier. The effective area curves and zero-points have been calibrated to high precision for the seven UVOT imaging bands. The ratio of exposure times is fixed by the operation of the CCD and the effective recharge time-scale for the MCPs has been determined in Section 4 ( $t_{\text{MCP}} = 0.236 \text{ ms}$ ); both of these quantities are independent of the imaging passband in question. Thus all the

**Table 2.** Zero-points for read-out streak photometry in full-frame or windowed mode, for a 16 pixel  $\times$  16 pixel aperture, in the seven UVOT imaging passbands. The zero-points are in the UVOT Vega magnitude system; for AB–Vega magnitude offsets see Breeveld et al. (2011).

Filter	Full-frame zero-point	Large-window zero-point	Small-window zero-point
UVW2	7.49	8.28	8.74
UVM2	6.96	7.75	8.21
UVW1	7.55	8.34	8.80
<i>u</i>	8.45	9.24	9.70
<i>b</i>	9.22	10.01	10.47
<i>v</i>	8.00	8.79	9.25
White	10.40	11.19	11.65

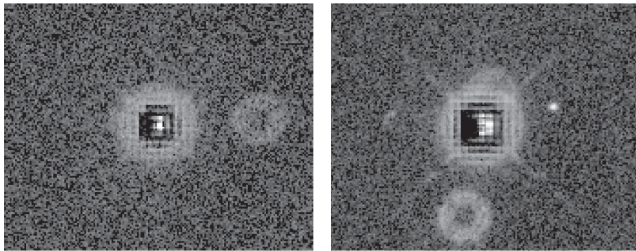


**Figure 7.** Identifying heavily saturated stars. The star on the left has a *v* magnitude of 9.3 and is suitable for read-out streak photometry, while the star on the right is of *v* magnitude 7.8, and is too bright for read-out streak photometry. Note the presence of diffraction spikes, the larger extent of the modulo-8 distorted region, and the crescent-like appearance of the core in the star on the right.

required elements are in place to enable read-out streaks to be used for photometric measurements in all the UVOT imaging passbands. Table 2 gives the zero-points for read-out streak photometry, determined from the standard imaging zero-points (Breeveld et al. 2011) and the ratio of the CCD integration and frame-transfer times. In Section 4 we showed that the read-out streaks produce good *v*-band photometry for sources from the detection limit of *v* = 12 up to *v* = 9, but in general one will not know the magnitude of the source a priori, so the bright-source threshold must instead be specified in terms of observed count rate in the read-out streak. Inspection of Fig. 5 suggests that coincidence-loss-corrected count rates up to  $0.3 \text{ s}^{-1}$  will produce robust photometry for full-frame imaging;<sup>4</sup> equivalent maximum count rates for the windowed modes are provided in Table 1. This bright-source limit is 2.4 mag brighter than the coincidence-loss limit for standard aperture photometry of a point source in full-frame imaging. We note that the large scatter in the read-out streak brightness for *v* < 8 means that some much brighter stars stray into the regime of count rates  $< 0.3 \text{ s}^{-1}$ . In practice, these very heavily saturated stars can be discriminated by their appearance, as illustrated in Fig. 7.

We outline our recommended procedure for obtaining photometry from read-out streaks in Appendix A and provide a brief discussion of the potential extension of the method to XMM-OM in Appendix B.

<sup>4</sup> Note that this cut-off in count rate, i.e. a horizontal line in Fig. 5, translates via Table 2 to a nominal bright limit of *v* = 9.31, which is more conservative than the bright limit of *v* = 9.0, discussed so far, for a *v* magnitude which is known a priori.

## 5.2 Photometric scatter

In the measurement of the read-out streaks outlined in Section 3.2, we estimated the uncertainties assuming Poisson statistics, purely on the measured number of counts within the read-out streak aperture. The uncertainty on the background was assumed to be negligible, as it was determined over a much larger number of columns than the measurement of the read-out streak. The Poisson errors were scaled by the same factor as the count rates in the coincidence-loss correction stage (equation 4). However, in Section 4 we found an additional systematic component to the photometric scatter between the Tycho-2 magnitudes and the UVOT read-out-streak magnitudes of around 0.1 mag after taking into consideration the uncertainties on the Tycho-2 magnitudes and the Poisson uncertainties on the read-out streak measurements. We can identify at least two sources of uncertainty which contribute to this additional scatter, and a third source that may. The first is inherent to the background determination. Usually one might assume that the background is intrinsically smooth on 16 pixel (8 arcsec) scales, and this would be a reasonable assumption for the genuine zodiacal background in the UVOT images. However, the column-by-column background also contains the read-out streaks of all the sources in the image, which will contribute genuine scatter on the scale of the 16 pixel aperture we have used to measure the read-out streaks. Secondly, the coincidence loss due to the MCPs changes the inherent uncertainties on the count rates in the read-out streaks from Poisson errors to binomial errors (Kuin & Rosen 2008), which are larger. Unfortunately, unlike the case considered by Kuin & Rosen (2008), the read-out streaks are superimposed on a significant background which is accumulated over a different time interval (during the integration of the static image) and for which MCP-related coincidence loss is negligible. Thus in the case of the measured read-out streaks, the uncertainties are neither pure Poisson nor pure binomial. Our recommended maximum count rate of  $0.3 \text{ s}^{-1}$  bright limit for read-out-streak photometry corresponds to 0.5 incident counts per MCP frame; comparison with fig. 1 of Kuin & Rosen (2008) shows that this limit corresponds to a binomial uncertainty which is 1.5 times as large as the Poisson error, so this is a significant effect. These two effects play off against each other: uncertainties in the background will produce the most significant photometric errors for faint read-out streaks, while the non-Poissonian nature of the errors induces photometric scatter primarily for bright read-out streaks. The third, potential, effect is that we do not have a measure of the uniformity of the MCP recharge time over the detector or its long-term evolution as the MCPs age. Any such variations in the recharge time of the MCPs will correspond directly to a scatter in the value of  $t_{\text{MCP}}$  which should be employed in the coincidence-loss correction, which will in turn induce photometric scatter in data which is corrected for coincidence loss assuming  $t_{\text{MCP}} = 0.236 \text{ ms}$ . Such an effect will produce photometric scatter which is largest for the brightest read-out streaks.

We do not have a theoretical prescription for any of these additional sources of photometric uncertainty, so we resort to the empirical estimate of the photometric scatter which is seen in addition to the simple Poisson errors. In keeping with the results presented in Fig. 6 and Section 4, we suggest that a systematic error of 0.1 mag is added in quadrature to all magnitudes derived from read-out streaks.

## 5.3 Verification in b

To verify the read-out streak photometry procedure and the photometric accuracy derived above, in a different UVOT band, we

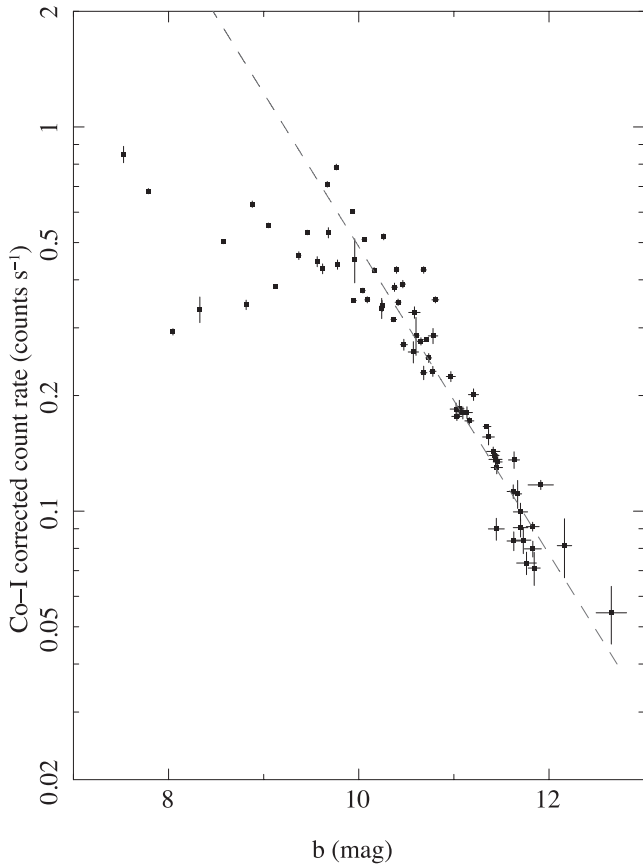


**Figure 8.** Count rates of the read-out streaks from Tycho-2 stars measured in the UVOT  $b$  band after correction for coincidence loss via equation (4) and  $t_{\text{MCP}} = 0.236$  ms. The dashed line corresponds to the predicted relation given in Section 2 based on the relative exposure times of the read-out streak and the static image.

move to the UVOT  $b$  band and once again make use of the Tycho-2 catalogue. The UVOT  $b$  band extends about  $400 \text{ \AA}$  to the red of the Tycho-2  $B_T$  band, so the transformation from  $B_T$  to  $b$  magnitude has a large colour term in  $B_T - V_T$ . Making use of the Pickles (1998) spectral library, we obtain the following transformation for stars with  $B_T - V_T > 0.4$ , excluding M stars.

$$b = B_T + 0.036 - 0.270(B_T - V_T). \quad (5)$$

The rms scatter of the data points about this relation is  $0.009$  mag. Stars with  $B_T - V_T < 0.4$  do not follow this relation.

We then measured the read-out streaks in the  $b$  band, following the procedure outlined in Appendix A, for a subset of the Tycho-2 stars described in Section 3.1, which have  $B_T - V_T > 0.4$  and which have  $b$  band observations with UVOT. This sample consists of 74 stars.

The coincidence-loss-corrected count rates are shown in Fig. 8 as a function of UVOT  $b$  magnitude, as derived from the Tycho-2 photometry. The data points follow closely the behaviour seen in the  $v$  band: they follow the relationship predicted from the ratio of the exposure times of the static image and the read-out streak for count rates below  $0.3 \text{ s}^{-1}$ , and deviate from this relationship increasingly at brighter magnitudes.

The throughput of UVOT is higher in  $b$  than in  $v$ , but the Tycho-2 photometry is less precise in  $B_T$  than in  $V_T$  (Høg et al. 2000), with the consequence that the dynamic range over which UVOT  $b$ -band

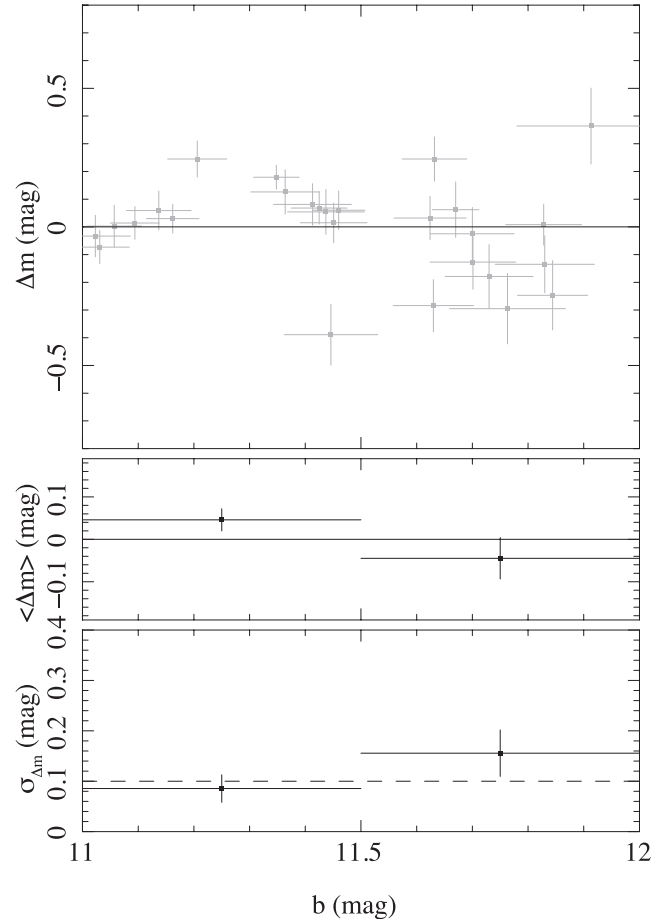


**Figure 9.** Top panel: differences  $\Delta m$  between the  $b$  magnitudes obtained from Tycho-2 and the  $b$  magnitudes obtained from the coincidence-loss corrected count rates of the UVOT read-out streaks. Uncertainties are the quadrature sums of the errors on the count rates and the Tycho-2 magnitudes. Middle and bottom panels: mean and dispersion of  $\Delta m$ , respectively, in  $0.5$  mag bins. The dashed line in the bottom panel shows the  $0.1$  mag systematic advocated in Section 5.2.

read-out streak measurements can be compared to magnitudes derived from Tycho-2 is considerably smaller than for the  $v$  band. Fig. 9 shows the differences between the  $b$  magnitudes derived from read-out streaks and the  $b$  magnitudes derived from Tycho-2 photometry, in the magnitude range for which the count rates are below  $0.3 \text{ s}^{-1}$ . Note that in this figure the  $0.1$  mag systematic error (see Section 5.2) has not been included in the uncertainties so that the magnitude of this systematic can be verified. As can be seen in this figure, there is no systematic offset between the predicted and observed read-out-streak magnitudes, and the systematic component of the uncertainty is consistent with the  $0.1$  mag derived in Section 5.2.

#### 5.4 Verification in UVM2

Although there is no comparable source of photometry to the Tycho-2 catalogue for the UVOT bands other than  $v$  and  $b$ , it is possible to verify that the read-out streaks produce viable photometry in the ultraviolet, for objects for which photometry can be synthesized using archival IUE spectra. The UVM2 band is the best UV band to perform this test because the response of UVM2 is almost completely contained within the IUE spectral range. In contrast UVW1

**Table 3.** Comparison of UVM2 magnitudes obtained from read-out streaks with synthetic magnitudes from IUE.

Star	Swift observation number	UVM2 from IUE (mag)	UVM2 from UVOT read-out streak (mag)
HD 168076	00044156001	$8.91 \pm 0.10$	$8.73 \pm 0.10$
HD 15570	00090050001	$10.45 \pm 0.10$	$10.44 \pm 0.10$

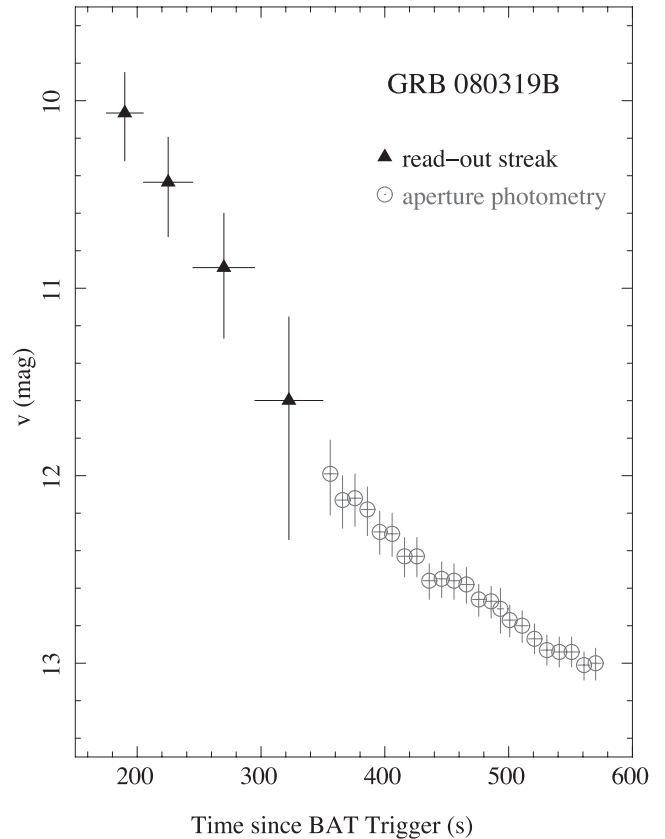
and UVW2 have red wings to their responses which extend beyond the long wavelength limit of IUE (see fig. 2 of Breeveld et al. 2011). The O stars HD 15570 and HD 168076 have suitable IUE spectra and have been observed in the UVM2 band with UVOT. Details of these two targets are provided in Table 3. The IUE large-aperture, low-resolution NEWSIPS spectra were obtained from the Mikulski Archive for Space Telescopes (MAST) and were combined to form a single spectrum per object. The spectra were then convolved with the UVM2 response to obtain synthetic magnitudes; the uncertainties on these magnitudes are dominated by systematics in the IUE spectra, which we assume to be 10 per cent (Massa & Fitzpatrick 2000). The read-out streaks from these two stars were measured using the procedures outlined above (including the 0.1 mag systematic error), and compared to the synthetic photometry from IUE. As seen in Table 3, the UVM2 magnitudes measured from the read-out streaks show good consistency with the synthetic magnitudes measured from IUE.

### 5.5 Demonstration: the naked eye GRB 080319B

GRB 080319B had the brightest optical afterglow of any GRB so far observed with *Swift*. The afterglow was sufficiently bright that the  $v$ -band event-mode UVOT data taken less than 350 s after the BAT trigger could not be used due to coincidence loss (Racusin et al. 2008). Here we show that the read-out streaks can be used to obtain photometry between 170 and 350 s after the trigger (i.e. from the beginning of the  $v$  finding-chart exposure until the afterglow is faint enough that normal aperture photometry can be used). The event mode data between 170 and 350 s were split into four time intervals, and in each time interval an image in raw coordinates was formed. In each image the read-out streak was measured following the procedure described in Appendix A. The photometry so derived is listed in Table 4, and shown together with the aperture photometry for the remainder of the finding-chart exposure, taken from the supplementary information of Racusin et al. (2008), in Fig. 10.

**Table 4.** Early-time UVOT  $v$ -band photometry of GRB 080319B measured from read-out streaks in images formed in raw coordinates from event-mode data. The first column,  $T - T_0$ , gives the mid-time of the image after the BAT trigger, and the second column gives the duration of the image.

$T - T_0$ (s)	Duration (s)	$v$ (mag)
190.0	30.0	$10.07^{+0.26}_{-0.22}$
225.0	40.0	$10.44^{+0.29}_{-0.24}$
270.0	50.0	$10.89^{+0.38}_{-0.29}$
322.5	55.0	$11.60^{+0.74}_{-0.45}$

**Figure 10.** Early-time UVOT  $v$ -band photometry of GRB 080319B. The triangles are measurements obtained from read-out streaks while the source is too bright to be measured from the direct image, and circles show the aperture photometry at later times from Racusin et al. (2008).

## 6 CONCLUSIONS

We have investigated the use of read-out streaks in obtaining photometric measurements of stars which are too bright for normal aperture photometry in MCP-intensified CCD detectors, and in particular the *Swift* UVOT. Our study is based on UVOT  $v$ -band measurements of stars in the Tycho-2 catalogue. We find that through the use of read-out streaks, photometric measurements can be obtained for stars up to 2.4 mag brighter than the usual coincidence loss limit. The read-out streaks, which are formed during the frame transfer on the CCD, are not affected by coincidence loss arising in the CCD. Instead, we find that coincidence-loss associated with the recharge time of the pores of the MCPs in the intensifier becomes significant. We calibrated the MCP coincidence loss using the Tycho-2 measurements. Our analysis of the photometric scatter in the read-out-streak measurements of Tycho-2 stars indicates that systematics and un-accounted sources of error limit the photometric precision to 0.1 mag over the factor of 10 dynamic range for which the read-out streaks are useful.

## ACKNOWLEDGEMENTS

This work was supported by the United Kingdom Space Agency (UKSA). We thank Rhaana Starling and Julian Osborne for useful discussions.

## REFERENCES

- Barthelmy S. D. et al., 2005, *Space Sci. Rev.*, 120, 143  
 Breeveld A. A. et al., 2010, *MNRAS*, 406, 1687  
 Breeveld A. A., Landsman W., Holland S. T., Roming P., Kuin N. P. M., Page M. J., 2011, *AIP Conf. Proc.* Vol. 1358, *Gamma Ray Bursts 2010*. Am. Inst. Phys., New York, p. 373  
 Burrows D. N. et al., 2005, *Space Sci. Rev.*, 120, 165  
 Eberhardt E. H., 1981, *IEEE Transactions on Nuclear Science*, 28, 712  
 ESA, 1997, in *ESA SP-1200, The Hipparcos and Tycho Catalogues*. ESA, Noordwijk  
 Fordham J. L. A., Bone D. A., Read P. D., Norton T. J., Charles P. A., Carter D., Cannon R. D., Pickles A. J., 1989, *MNRAS*, 237, 513  
 Fordham J. L. A., Kawakami H., Michel R. M., Much R., Robinson J. R., 2000a, *MNRAS*, 319, 414  
 Fordham J. L. A., Moorhead C. F., Galbraith R. F., 2000b, *MNRAS*, 312, 83  
 Gehrels N., 2004, *ApJ*, 611, 1005  
 Høg E. et al., 2000, *A&A*, 355, L27  
 Johnson H. L., Morgan W. W., 1951, *ApJ*, 114, 522  
 Kawakami H., Bone D., Fordham J., Michel R., 1994, *Nucl. Instrum. Methods Phys. Res. A*, 348, 707  
 Kuin N. P. M., Rosen S. R., 2008, *MNRAS*, 383, 383  
 Maccacaro T., Gioia I. M., Wolter A., Zamorani G., Stocke J. T., 1988, *ApJ*, 326, 680  
 Mason K. O. et al., 2001, *A&A*, 365, L36  
 Massa D., Fitzpatrick E. L., 2000, *ApJS*, 126, 517  
 Pickles A. J., 1998, *PASP*, 110, 863  
 Poole T. S. et al., 2008, *MNRAS*, 383, 627  
 Racusin J. L. et al., 2008, *Nat*, 455, 183  
 Roming P. W. A. et al., 2005, *Space Sci. Rev.*, 120, 95  
 Skrutskie M. F. et al., 2006, *AJ*, 131, 1163  
 Talavera A., 2011, Technical Report XMM-SOC-CAL-TN-0019 Issue 6.0, *XMM-Newton Optical and UV Monitor (OM) Calibration Status*, ESA; available at: <http://xmm2.esac.esa.int/docs/documents/CAL-TN-0019.pdf>

## APPENDIX A: RECOMMENDED PROCEDURE FOR OBTAINING PHOTOMETRY FROM READ-OUT STREAKS

(i) Mask the raw image from bright sources, and mask fainter sources on a column-by-column basis so that the read-out streaks are preserved (see Section 3.2 for more detailed recommendations regarding masking).

(ii) Measure the mean counts per non-masked pixel in each column and scale to a 16 row aperture.

(iii) Identify the columns containing the read-out streak of interest and measure its count rate in a 16-pixel aperture, subtracting a suitable background estimate. Estimate the uncertainty on the count rate assuming Poisson statistics.

(iv) Correct the count rate for coincidence loss using equation (4) with  $t_{\text{MCP}} = 0.236$  ms and the appropriate value of  $S$  from Table 1. Scale the uncertainty by the same factor as the count rate.

(v) Check that the coincidence-loss corrected count rate is below the maximum recommended count rate given in Table 1, and the star is not heavily saturated (see Fig. 7). We only recommend that photometry is derived from the read-out streak if these conditions are satisfied.

(vi) Apply the large-scale sensitivity correction according to the position of the star within the image,<sup>5</sup> and the time-dependent sensitivity correction<sup>6</sup> appropriate to the time of the UVOT observation (Breeveld et al. 2010) to the coincidence-loss corrected count rate and its uncertainty.

(vii) Obtain a magnitude and associated uncertainty from the coincidence-loss corrected count rate and its uncertainty using

$$M = ZP - 2.5 \log_{10} R_i$$

where  $M$  is the magnitude,  $R_i$  is the coincidence-loss corrected count rate and  $ZP$  is the zero-point given in Table 2 for the relevant UVOT passband and window mode.

(viii) Add in quadrature a systematic uncertainty of 0.1 mag to the statistical uncertainty on the magnitude.

## APPENDIX B: POTENTIAL EXTENSION TO XMM-OM

The principles for obtaining read-out-streak photometry outlined in this paper are expected to apply equally to XMM-OM, though we caution that we have not verified experimentally any aspect of read-out-streak photometry with XMM-OM. XMM-OM is operated with different frame times to UVOT, but the frame-transfer time is the same, so the ratio of exposure times of the static image to the frame-transfer  $S$  is easily calculated for the XMM-OM frame times. Using  $S$ , and the calibrated zero-points for normal aperture photometry (Talavera 2011), zero-points appropriate for read-out streak photometry with XMM-OM can thus be derived in an identical fashion to the zero-points presented here for UVOT. The only experimentally determined parameter in the transformation of UVOT read-out streak measurements to photometry is the effective recharge time of the MCP,  $t_{\text{MCP}}$ . This time-scale is expected to depend on the product of the recharge resistance and the capacitance per channel of the final-stage MCP, which in turn will depend on its physical characteristics such as material, dimensions and pore layout (Eberhardt 1981). The MCPs used for the UVOT and XMM-OM have identical specifications and were procured in the same time period from the same manufacturer, the UVOT MCPs being spares from the development of XMM-OM. Therefore our expectation is that the effective recharge time-scale of the XMM-OM MCP should be very similar to the  $2.36 \times 10^{-4}$  s measured for the UVOT MCP.

<sup>5</sup> In the calibration data base (CALDB) used by the standard *Swift* FTTOOLS (<http://heasarc.gsfc.nasa.gov/docs/heasarc/caldb/data/swift/uvota>) this correction is contained within the file `swulssens20041120v003.fits` (where v003 refers to the version number and will be incremented as the calibration is updated).

<sup>6</sup> In the CALDB used by the standard *Swift* FTTOOLS this correction is contained within the file `swusenscorr20041120v003.fits` (where v003 refers to the version number and will be incremented as the calibration is updated).

This paper has been typeset from a  $\text{\TeX}/\text{\LaTeX}$  file prepared by the author.